UCRL- 92598 Rev. 1
PREPRINT

INSTABILITIES, TURBULENCE, AND THE PHYSICS OF FIXED POINTS

Minh Duong-van
University of California
Lawrence Livermore National Laboratory
Livermore, CA 94550

Submitted to
Phys. Rev. Lett.

July 1985

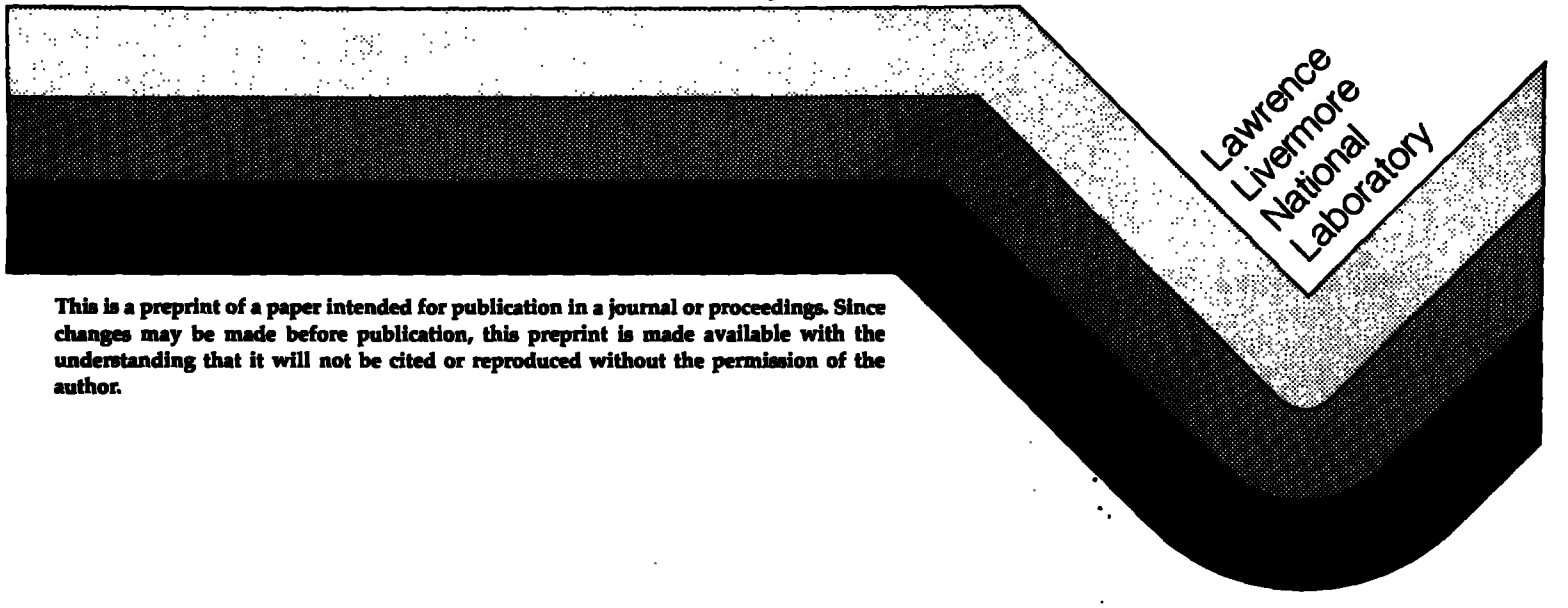

DISCLAIMER

INSTABILITIES, TURBULENCE, AND THE PHYSICS OF FIXED POINTS*

Minh Duong-van

University of California

Lawrence Livermore National Laboratory

Livermore, CA 94550

ABSTRACT

By solving the recursion relation of a reaction-diffusion equation (involving a quadratic map and nearest-neighbor contributions) on a lattice, we find two distinct routes to turbulence, both of which reproduce commonly observed phenomena: the Feigenbaum route, with period-doubling frequencies, which eventually leads to chaotic turbulence with a flat Fourier spectrum; and a much more general route with noncommensurate frequencies and frequency entrainment, and locking, which eventually leads to a Kolmogorov-type ($f^{-5/3}$) spectrum. Intermittency and large-scale aperiodic spatial patterns, also observed in physical systems, are reproduced in this new route. We discuss the entropy flows connected with the recursion relation, and note a similarity between the underlying physics of the patterns generated in our simulations and the physics of the Prigogine dissipative structures.

*Work performed under the auspices of the U.S. Department of Energy by the Lawrence Livermore National Laboratory under contract number W-7405-ENG-48.

Experimental evidence supporting Feigenbaum's route to turbulence[1,2] has become richer since 1978. In this route, nonlinear systems manifest chaos via period- doubling bifurcations. For example, Rayleigh-Bénard systems with low[3-5] and intermediate[6] Prandtl numbers exhibit this route. In detailed experiments on low- aspect-ratio Rayleigh-Bénard cells, Giglio et al.[6] saw four period doublings and obtained values of δ that agree with Feigenbaum's[1] universal $\delta = 4.6692$ within their experimental error.

When the aspect ratio is large, however, very different behavior is found.[7-11] As the stress parameter (the Rayleigh number, in the case of Rayleigh-Bénard systems) is increased, cascades of instabilities are observed, each step of which adds new complications to the convective behavior.[3,8,10] Unstable patterns are formed and temporal chaos[8] sets in, with alternating random bursts and quietness: this is called intermittency.[3,8] Noncommensurate frequencies arise in the Fourier spectrum of the chaotic variable, and entrainment and locking occur as the stress parameter is varied.[3,7,8]

In this paper we show that both these routes to turbulence, with all the properties just described, can be simply simulated with a quadratic map at each site of a spatial lattice and with a coupling between nearest-neighbor sites. Our most significant result is that this new route leads to a Kolmogorov-type turbulence,[12,13] with $P(f) \propto f^{-5/3}$, where the exponent 5/3 is shown to be a consequence of a quadratic map.

Let u represent the chaotic variable: it may be a velocity component or a temperature fluctuation of the system being studied. We build a lattice of sites with a quadratic map $u \rightarrow Q(\lambda,u)$ at each site, and allow interaction between nearest neighbor sites through a coupling parameter g. We assign a random value of u to each lattice site, and let the lattice evolve in time steps $t_n = n\tau$, $n = 1, 2, 3, \ldots$, where τ is the Poincaré time of the system. We find the same behavior for all quadratic $Q(\lambda,u)$: for example,

$$Q(\lambda,u) = \lambda u(1-u)\,, \tag{1a}$$

$$Q(\lambda,u) = \lambda \sin(\pi u) \tag{1b}$$

give the same behavior. For simplicity, we use the logistic map, Eq. (1a), in this study. In one dimension, we use the prescription[14,15]

$$u_{n+1}(m) = \lambda u_n(m)[1-u_n(m)] + \frac{g}{2}[u_n(m+1) + u_n(m-1) - 2u_n(m)]\,, \tag{2}$$

where the index m spans the N lattice points m = 1, 2, ..., N. Similarly, in two dimensions we have

$$\begin{aligned} u_{n+1}(j,k) = {} & \lambda u_n(j,k)\,[1-u_n(j,k)] \\ & + \frac{g}{4}[u_n(j+1,k) + u_n(j-1,k) - 2u_n(j,k)] \\ & + \frac{g}{4}[u_n(j,k+1) + u_n(j,k-1) - 2u_n(j,k)]\,, \end{aligned} \tag{3}$$

where the indices j, k span the lattice in the x and y directions, respectively.

With Eq. (2) [the same results are found for Eq. (3)], two routes to turbulence are observed, in which the Feigenbaum route is seen as a special case.

For small g (e.g., $g \simeq 0.001$), when λ approaches the accumulation point λ_∞, the Fourier spectrum of the time sequence $u_n(m)$ for a particular m shows period-doubling bifurcations.[1] (With $\lambda_\infty \simeq 3.569$ and $g \simeq 0$, for example, we obtain a period-doubling Fourier spectrum that agrees well with that obtained by Giglio et al.[6]) As g increases, the peaks in the Fourier spectrum become wider, as observed by Mauer and Libchaber.[3] In our study, this width increase is a consequence of the dissipative term controlled by g. As λ increases to 4 (for <u>any</u> value of g) the spectrum becomes flat and chaotic.

Only in special cases (such as in Rayleigh–Bénard systems with low aspect ratio) does the turbulence observed in nature follow the Feigenbaum route. More generally (as in Rayleigh–Bénard systems with large aspect ratios), the instabilities and turbulence show richer behaviors.[7–11] One observes noncommensurate frequencies in the Fourier spectrum and the phenomena of frequency entrainment and locking; complex quasi–periodic, aperiodic, and intermittent time histories of the values of chaotic variables at individual points in the system; and similar time variations in the spatial patterns formed in certain systems.[3] By iterating Eq. (2) or (in the case of the spatial patterns) Eq. (3) with values of g away from zero, we can reproduce all these phenomena, provided we restrict λ to the Feigenbaum simple fixed points region $1 < \lambda < 3$.

We built a periodic one–dimensional lattice with N = 2000, and recorded the time evolution and the corresponding Fourier transform of u_n^{13} for times up to $n = 2^{12}$ and for a variety of values of λ and g (m is arbitrarily chosen equal to 13). We found that for every value of g, there is a λ_{max} at which the u eventually blows up (diverges) with time n. Parametrizing λ_{max} as a function of g, we obtain an approximate relation $\lambda_{max} = a - bg$, where a and b are positive quantities whose values depend on the lattice site observed.

For illustration, we choose g = 0.915 and vary λ from $\lambda_{max} = 1.621$ to $\lambda_{min} = 1.0$. Figure 1(a) ($\lambda = 1.62$) shows the Fourier spectrum and the time history of u_n. This broad spectrum, with its intermittent bursts and quietness, appears to correspond to observations described in Ref. 3. In Fig. 1(b) ($\lambda = 1.52$) the frequency peaks become narrower, and the amplitude variations become smaller.

In Fig. 2(a) ($\lambda = 1.449$), the time history shows that the system attempts to settle to the fixed point ($u^* = 1 - 1/\lambda$) after some transient time. The competition between the approach to the fixed point (due to λ) and the diffusion away from the fixed point (due to

g) gives rise to the instability observed. In Fig. 2(a) ($\lambda = 1.449$) the Fourier spectrum exhibits noncommensurate frequencies, as observed by Mauer and Libchaber.[3]

As λ is decreased further, the frequencies are entrained (Fig. 2(b) $\lambda = 1.49$) and locked (Fig. 3(a) $\lambda = 1.48$).

The most interesting results are shown in Fig. 3(b) ($\lambda = 1.00$). The spectra manifest Kolmogorov-like behavior [$P(f) \propto f^{-\kappa}$, with $\kappa \simeq 5/3$]. This type of smooth power spectrum is observed when the system successfully approaches the fixed point. Note that for $\lambda \simeq 1$ and $g = .915$, κ is slightly greater than 5/3.[16] We found, in Table 1, $\kappa \simeq 1.66$ only at $\lambda = 1$ and $g = 0$.

We generate visible patterns with the two-dimensional Eq. (3) by use of a new graphical technique,[17] scaling the u(j, k) to a 0-to-256 linear gray scale. Simulations of this sort correspond quite closely to the patterns seen by Dubois and Bergé[8] in their experiments with silicon oil.

In the simulation of these patterns, the u(j, k) are assigned initial (n = 1) random values between 0 and 1, resulting at most in small-scale random patterns at that time. As time increases, these patterns disappear into a highly uniform sea (when u_n approaches the fixed point); eventually, however, large-scale structures grow, evolve, and temporarily or permanently stabilize. Fig. 4 shows the pattern developed in a 50x50 lattice for $\lambda = 1.5$, $g = .905$.

We have chosen to study only the simple fixed points region $1 < \lambda < 3$ of the logistic map, Eq. (2a). As long as $g = 0$, this branch produces uninteresting behavior: the u_n approach the fixed point $u^* = 1 - 1/\lambda$. Without g, there is no instability in this region, and no patterns. When we turn g on, however, depending on the values of g and λ, we may we get rich and interesting behaviors clearly, in Figs. 1 and 2, g acts to keep the u_n from their tendency toward the fixed point. Thus instabilities appear to result from a competition between tendencies towards the fixed points and away from it, and the time history intermittency phenomenon (Fig. 1a) is, in fact, a consequence of this competition.

In the region $1 < \lambda < 3$ of the logistic map, the Lyapunov exponent is negative, as is the corresponding entropy flow. However, the dissipative term g gives a positive entropy flow for large enough g. The competition between these two entropy flows gives rise to pattern formation. In an open system, the change of entropy is expressed by the sum of the entropy produced inside the system d_iS, and the entropy supplied externally or given off to the surroundings, d_eS:

$$dS = d_iS + d_eS$$

The quantity d_iS is always positive according to the second law of thermodynamics. The quantity d_eS depends on the exchange of heat, matter and charge between the system and its environment. In our model, the lattice represents an open system. At each iteration we apply a recursion relation that comprises two terms: a diffusion term represented by nearest neighbors coupling, and a nonlinear driving term, represented by a quadratic map. The lattice is started with random u's and the entropy of the lattice system is large. As the time n increases, for specific values of λ and g, patterns are formed and the entropy changes accordingly. Thus, we can regard recursion relations of the form of Eqs. (2) and (3) as the simplest mechanisms for introducing entropy changes into the lattice, which in this case is an open system, at each iteration.

We now discuss the critical exponent κ in the power spectrum $P(f) \propto f^{-\kappa}$. In many aspects, critical and chaotic phenomena manifest scaling and universality.[19] In critical phenomena, the order of phase transition reflects the physics of the system at the critical point. In chaotic phenomena, it is perhaps the order p of the critical point that determines the universal metric properties[1] represented by δ and α. Following the approach of Hu and Satija,[20] we determine δ and α from a generalized logistic map, $u_{n+1} = \lambda u_n(1 - u_n^p)$. Table 1 shows δ, α, and κ for several values of the exponent p.

Experimental data[21] show that $p = 1$ is preferred. In this study, we calculated κ as a function of p for the trivial fixed-point case ($\lambda = 1$). The fact that $\kappa \simeq 1.66$, very close to $\kappa = 5/3$ measured by Champagne in wind tunnel experiments,[18] again confirms the quadratic nature of the map used. It is tempting to enlarge the set δ, α of universal constants of the logistic map to include κ, and to postulate that this κ is the Kolmogorov exponent.

In conclusion, we note that the variety of phenomena experimentally observed in the approach to turbulence has brought forth a variety of explanations: for example, intermittency can be explained[22] by the Lorenz model; the lock-in phenomenon can be explained by the Flaherty and Hoppensteadt model.[23] In our model, by putting the quadratic map on the lattice with nearest neighbors coupling, we economically recover all these phenomena.

The author thanks P. R. Keller for the graphics used in this paper and P. W. Murphy for editorial assistance. He thanks his colleagues at Lawrence Livermore and Los Alamos National Laboratories for numerous profitable discussions. He also thanks the Aspen Institute for Physics for their hospitality and the participants for stimulating discussions.

REFERENCES

1. M. J. Feigenbaum, Phys. Lett. 74A, 375 (1979).
2. M. J. Feigenbaum, Comm. Math. Phys. 77, 65 (1980).
3. J. Mauer and A. Libchaber, J. Phys. Lett. 40, L–419 (1979); and Universality in Chaos, P. Cvitanovic, Ed. (Adam Hilger Ltd., Bristol, England, 1984), p. 109.
4. A. Libchaber and J. Mauer, J. Phys. Colloq. 41, C3–S1 (1980).
5. P. S. Linsay, Phys. Rev. Lett. 47, 1349 (1981).
6. M. Giglio, S. Musazzi, and V. Perini, Phys. Rev. Lett. 47, 243 (1981).
7. J. P. Gollub and S. A. Benson, Phys. Rev. Lett. 41, 948 (1978).
8. M. Dubois and P. Bergé, J. Fluid. Mech. 85, 641 (1978), and Systems Far From Equilibrium, L. Garrido, Ed. (Springer–Verlag, New York, 1980), p. 381.
9. G. Ahlers and R. W. Walden, Phys. Rev. Lett. 44, 445 (1980); Phys. Lett. 76A, 53 (1980).
10. G. Ahlers and P.R. Behringer, Supp. Prog. Theor. Phys. 64, 186 (1978).
11. J. Mauer and A. Libchaber, J. Phys. Lett. 41, 515 (1980).
12. A. N. Kolmogorov, Dokl. Akad. Nauk SSSR 30, 301 (1941); J. Fluid Mech. 13, 82 (1962).
13. F. H. Champagne, J. Fluid Mech. 86, 67 (1978).
14. K. Kaneko, Prog. Theor. Phys. 69, 1427 (1983); Prog. Theor. Phys. 72, 480 (1984).
15. I. Waller and R. Kapral, Phys. Rev. A 30, 2047 (1984).
16. The turbulence intermittency μ can be extracted from the relation: $\kappa = 5/3 + \mu/3$, and μ is a small, positive number (experimentally $0<\mu<.5$).
17. Minh Duong–van and P. R. Keller, "Pattern Formation in Spinodal and Phase Turbulent Instabilities," Lawrence Livermore National Laboratory, Livermore, CA, UCRL–92716 (1985).

18. P. Glansdorff and I. Prigogine, Thermodynamic Theory of Structure, Stability, and Fluctuations (Wiley-Interscience, New York, 1971).

19. B. Hu, Phys. Repts. 91. 233 (1982).

20. B. Hu and I. I. Satija, Phys. Lett. 98A, 145 (1983).

21. I thank P. Cvitanovic for providing me with information on a more comprehensive survey of recent data on this phenomenon. Also, Universality in Chaos, P. Cvitanovic, Ed. (Adam Hilger Ltd., Bristol, England, 1984), p. 29.

22. P. Berge, M. Dubois, P. Mannville and Y. Pomeau, J. Physique-Lettres 41, L-341 (1980).

23. J. E. Flaherty and F. C. Hoppensteadt, Study Appl. Math., 58, 5 (1978).

Table 1. Values[20] of the Feigenbaum δ and α, and of our power spectrum exponent κ, for various values of p in the generalized logistic map $u_{n+1} = \lambda u_n(1 - u_n^p)$.

p	δ	α	κ
0	2	∞	0
1	4.6692	2.5029	1.66
2	6.0847	1.9277	1.93
3	7.2851	1.6903	1.96
10	13.15	1.27	1.99

FIGURE CAPTIONS

Figure 1. (Top to bottom: Fourier spectrum of u_n; u_n; and enlargement of indicated portion of u_n.) (a) $g = 0.915$, $\lambda = 1.62$; (b) $\lambda = 1.52$.

Figure 2. (Same plots as in Fig. 1.) (a) $g = 0.915$, $\lambda = 1.499$; (b) $\lambda = 1.490$.

Figure 3. (Same plots as in Fig. 1.) (a) $g = 0.915$, $\lambda = 1.48$; (b) $\lambda = 1.00$.

Figure 4. Patterns generated by a 50 x 50 lattice with $\lambda = 1.50$, $g = .905$ and $n = 90$.

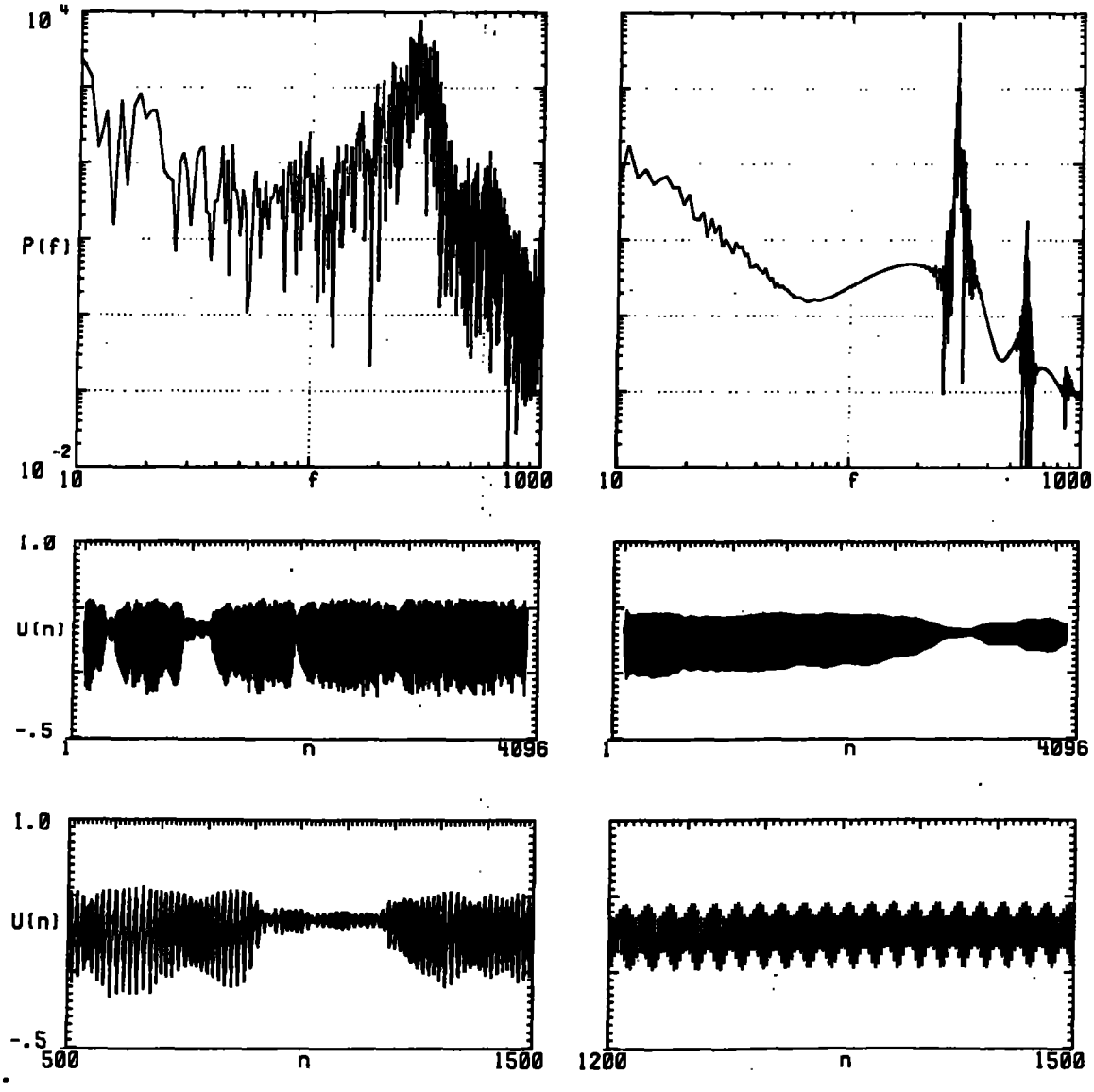
10 4
P(f)
10 -2
10
f
1000
1.0
U(n)
-.5
1
n
4096
1.0
U(n)
-.5
500
n
1500
10
f
1000
1
n
4096
1200
n
1500

Fig. 1a

Fig. 1b

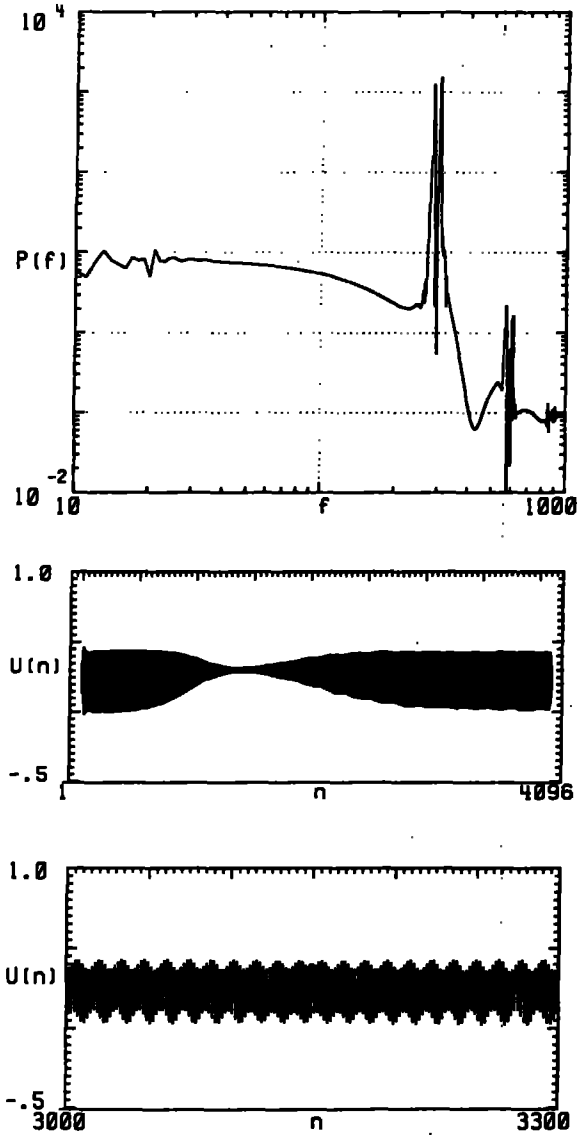
10 4
P(f)
10 -2
10
f
1000
1.0
U(n)
-.5
1
n
4096
1.0
U(n)
-.5
3000
n
3300

Fig. 2a

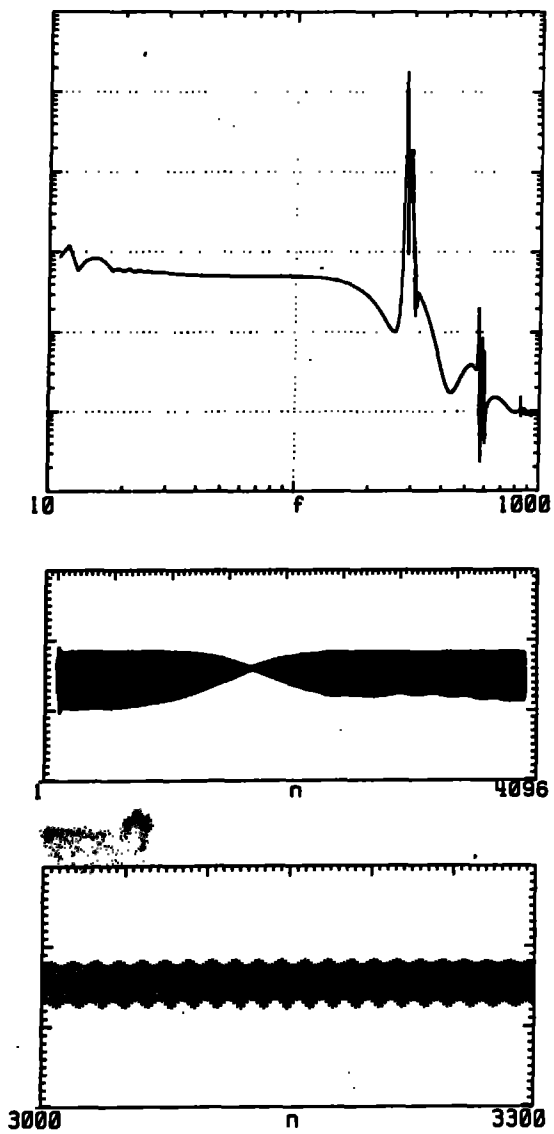
10
f
1000
1
n
4096
3000
n
3300

Fig. 2b

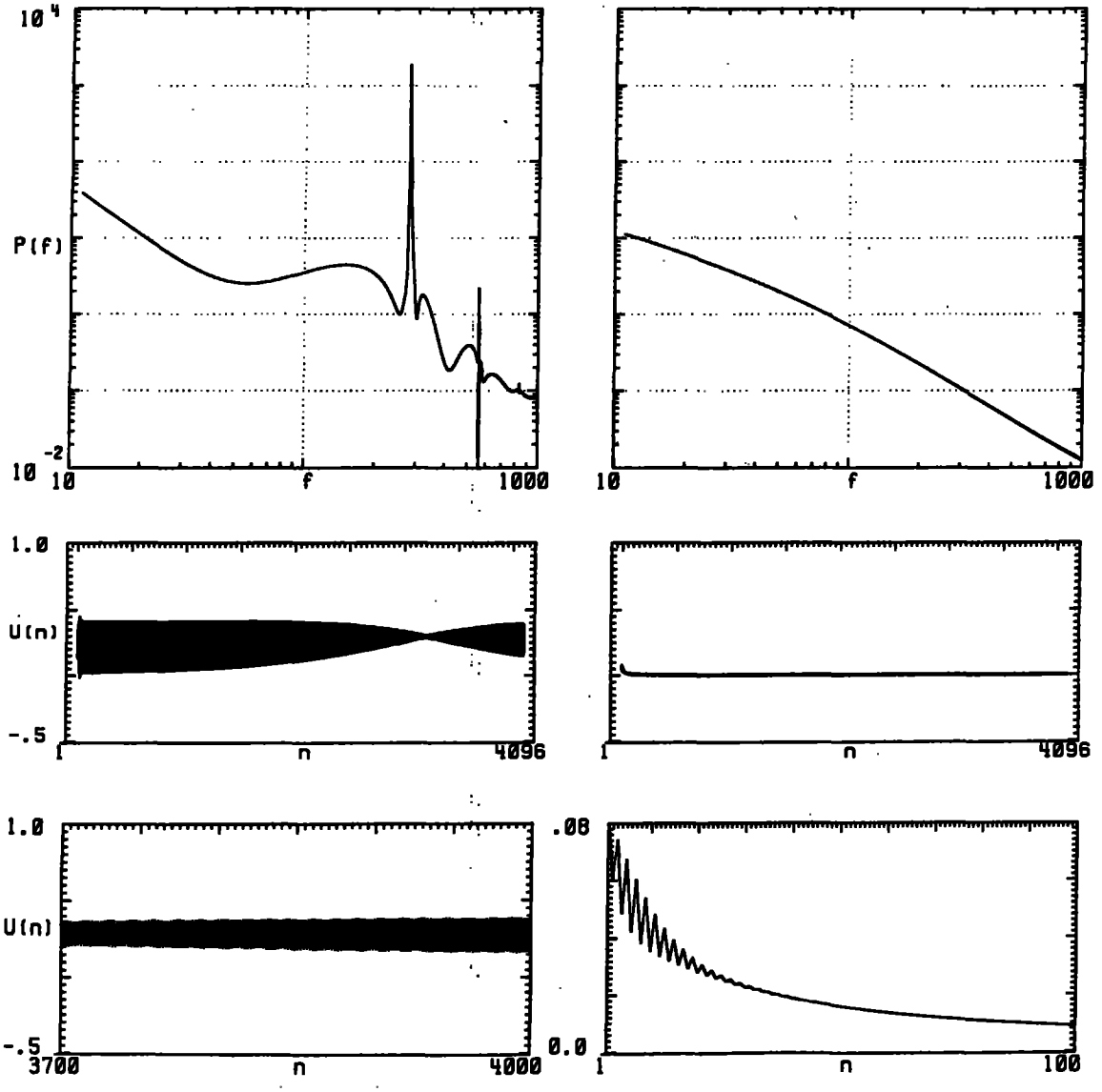

Fig. 3a

Fig. 3b

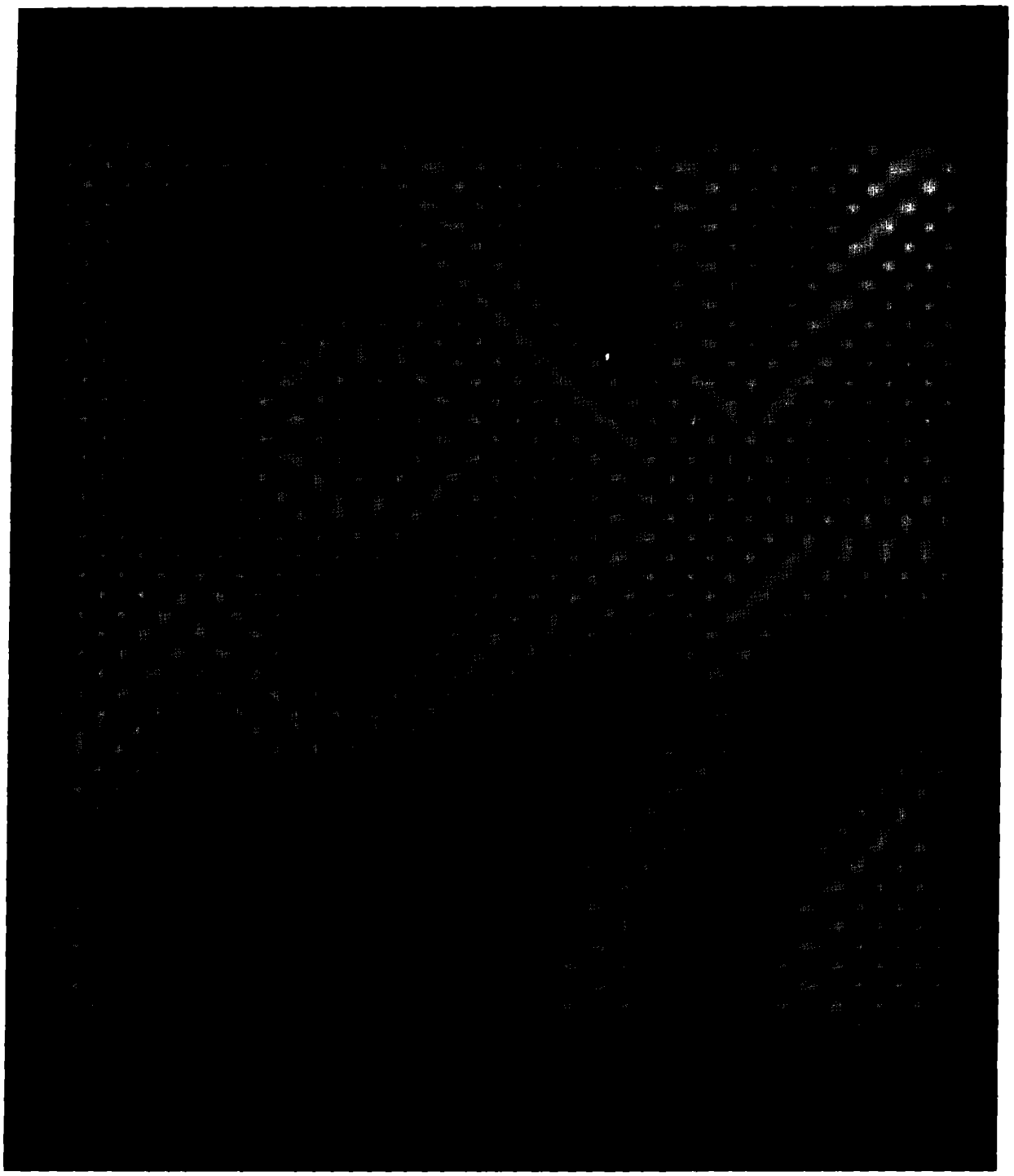

Fig. 4